Title

A methodology for generating reduced-order models for large-scale buildings using the Krylov subspace method

Journal

Journal of Building Performance Simulation, 13(4)

ISSN

1940-1493

Authors

Kim, Donghun
Bae, Yeonjin
Yun, Sehyun
et al.

Publication Date

2020-07-03

DOI

10.1080/19401493.2020.1752309

Peer reviewed

To appear in the *Journal of Building Performance Simulation*
Vol. 00, No. 00, Month 20XX, 1–19

A Methodology for Generating Reduced-Order Models for Large-Scale Buildings using the Krylov Subspace Method

Donghun. Kim[a,b] *, Yeonjin Bae[a,c], Sehyun Kim and James.E. Braun[a]

[a] *Ray W. Herrick Laboratories, Purdue University, IN, USA*
[b] *Energy Technologies Area, Lawrence Berkeley National Laboratory, CA, USA*
[c] *Buildings Integration and Controls Research, Oak Ridge National Laboratory, TN, USA*

(*Received 00 Month 20XX; final version received 00 Month 20XX*)

Developing a computationally efficient but accurate building energy simulation (BES) model is important in order to accelerate building design optimizations, retrofit analysis, and development and evaluation of advanced control algorithms where a number of iterations over a long simulation period are required. For this purpose, identification approaches that develop simplified models from building simulation datasets could replace detailed energy simulation software. However, those approaches require extensive computational time at the front to generate necessary data sets and train models for sufficient reliability. An alternative approach that utilizes model order reduction (MOR) methods to directly extract a lower dimensional model from a detailed physics-based model consisting of a number of differential equations is attractive to avoid the pre-simulation requirement. Among many MOR approaches, the balanced truncation method has been most reliably and popularly applied to the building science field. However, it can not be practically applied to a large-scale building with many zones due to computational and data storage requirements. To overcome the problem, this paper introduces the Krylov subspace method to the building science field. Technical issues of applying the Krylov subspace method to building applications are addressed and a suitable algorithm that overcomes those challenges is presented. To demonstrate reliability of the algorithm, comparisons between the resulting reduced-order model (ROM) and a high fidelity model developed from a commercially available BES software for a 60-zone case study building are provided. The ROM was a factor of 100 faster than the high fidelity model but with high accuracy.

Keywords: building simulation, building load, reduced order model, Krylov subspace method, model order reduction

1. Introduction

The building sector consumes up to 40% of total energy consumption and 70% of electrical energy in many developed countries. Developing models which predict accurate dynamics of building loads and zone air temperatures are important for investigating more energy efficient solutions for buildings through building design optimization, retrofit analysis, sensitivity and uncertainty analysis, and real-time building control.

High fidelity building simulation tools, such as TRNSYS (Klein et al. 2004) and EnergyPlus (Crawley et al. 2000), calculate building performance based on solution of thousands of equations for each computation time step even for a medium-sized building. As a result, the direct usage of the high fidelity tools might be restricted for some practical applications, such as design and control optimization, particularly when a number of iterations of monthly or annual simulations are required. Therefore, computationally efficient but accurate building simulation models that could

*Corresponding author. Email: donghunkim@lbl.gov

replace high fidelity building simulation models are useful to accelerate those applications.

Many researchers have investigated data-driven modeling approaches (gray- or black-box modeling approaches) utilizing classical statistical methods, system identification or machine learning techniques to replace detailed energy simulation software: Refer to review papers of Foucquier et al. (2013); Li and Wen (2014) for various data-driven modeling methods and applications. However, these inverse modeling approaches require extensive computational time on the front end to generate the necessary data sets for training the model to ensure both reliability and high accuracy.

An alternative approach, namely model order reduction (MOR), that converts a high dimensional dynamic model to a reduced-order model (ROM) is attractive, since it completely bypasses the pre-simulation requirement for training by exploiting information contained in an original dynamic model. Many MOR techniques including the proper orthogonal decomposition, balanced realization method, singular perturbation method and moment matching approximation have been developed and investigated in the fields of computational fluid dynamics, mathematics, and control. See Antoulas et al. (2001) for a MOR survey paper and Antoulas (2005) for theoretical details.

Many studies of MOR methods applied to buildings can also be found in the literature. Palomo et al. (1997) investigated several state transform methods to select a suitable reduction technique for thermal building models. The authors also applied a MOR method to design an optimal controller (Palomo Del Barrio et al. 2000). In the paper, a reduced-order linear time invariant (LTI) model for a multi-zone building was developed from a detailed description of the wall dynamics based on a finite volume or finite difference method. Ménézo et al. (2002) proposed a state aggregation method which develop a lower dimensional model for each wall and construct a multi-zone model from the reduced wall models. Deng et al. (2010) proposed a method to reduce complicated thermal networks by aggregating a number of nodes into "super-nodes". The proposed method is based on model reduction of Markov chains. Goyal and Barooah (2012) also started from a simplified wall model for wall dynamics described as 3R2C (three resistances and two capacitances) in order to obtain a reduced-order zone model. A multi-zone model is constructed from the simplified wall models and then a balanced truncation method is applied to further reduce the dimension. A model-order reduction method to treat nonlinearities appearing from water vapor balance equations was also presented. Picard et al. (2017) utilized the balanced truncation method to have a reduced order building envelop model to construct and test performance of a model predictive controller (MPC).

Among the variety of MOR techniques applied to buildings, the balanced truncation method (Moore 1981) could be one of the most reliable and popular methods when a system behaves linearly[1] (Palomo et al. 1997; Goyal and Barooah 2012; Kim and Braun 2015; Del Barrio et al. 2000; Plessis et al. 2011; Gao et al. 2008; Picard et al. 2017; Ioli et al. 2017). The method calculates the singular values of the *Hankel* operator determined by *balancing* the *observability* and *controllability* gramians of an original linear time invariant (LTI) system. Then, dynamic states that are hardly controllable and hardly observable detected by the singular values are truncated. Compared with other MOR methods, it has unique features that are 1) the generated ROM preserves original system properties, such as stability, controllability and observability, and 2) it provides a way of estimating truncation errors for a ROM.

Despite the desired characteristics of the balanced truncation method, the computational cost to generate a ROM is significant, because the balancing process needs to solve two matrix equations, i.e. the *Lyapunov* equations of the full-order system of which computation cost for generating a ROM increases with $O(n^3)$ where n is the state dimension (Laub 2005). For a large-scale building such as schools, office buildings, multi-family apartments, it is not unusual to have the state dimension higher than 10^3. For example, consider a 30-zone building where each zone has 6 surfaces and each surface consists of an average of 3 different wall layers (materials). With two temperature nodes for each layer, the state dimension for the building becomes at least $1110 = (30 \times (6 \times 3 \times 2 + 1))$.

[1]Although some authors argue that the bilinear term for the heat flow in the zone air energy balance makes a building system nonlinear and hence a number of available linear MOR techniques is limited for building applications (Deng et al. 2014), it is not true since it becomes linear when the bilinear term is treated as an input to the system.

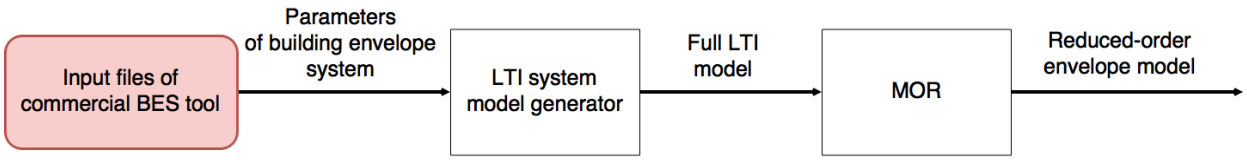

Figure 1. Proposed MOR approach

Since the computation time for the balanced truncation method increases cubically with the state dimension, it may not be feasible to apply the MOR method for large-scale buildings, especially when parametric studies or optimization for design are needed.

Surprisingly, very few MOR methods that can systematically handle high dimensional buildings have been to the building energy simulation field. In this paper, we introduce a MOR method, i.e. *the Krylov subspace method*, as an alternative to the balanced truncation method for large-scale building applications. Technical issues of applying the Krylov subspace method to buildings are addressed and a general algorithm to overcome the challenges is developed and presented. To demonstrate its reliability and high performance, comparisons of building load predictions and computational requirements to a high fidelity model from a commercial BES software for a 60-zone building are provided.

2. System of Interest

In this paper, we are considering dynamics of building envelope systems that map to building loads or zone air temperature profiles from internal heat gains and weather conditions. Building HVAC systems are excluded in this paper, since they are typically modeled with nonlinear algebraic equations which are out of the scope of general MOR methods. To complete building energy simulations, a ROM for a building envelope system should be coupled to a building HVAC system. We refer to the paper of Kim et al. (2013) for a case study of integrated ROM and HVAC models.

3. Methodology

The overall approach that we are proposing to obtain a ROM for a building envelope system as an alternative to data-driven approaches is depicted in Figure 1. It starts from extracting physical parameters of a building envelope system, such as wall layer (material) properties, layer composition for a wall and wall tilt/azimuth angles, from an input file of a commercial BES tool, e.g. *.bui for TRNSYS and *.idf for EnergyPlus. Then, a full thermal network model for the building envelope system is constructed based on the data. The full model is passed to a MOR algorithm to generate a ROM. Since MOR algorithms do not require simulations with a computationally heavy model for training but only requires matrix operations, the approach fundamentally differs from any data-driven approaches.

Although the main focus of this paper is on a MOR algorithm, it is necessary to describe the LTI (linear time invariant) system model generator in the figure. This is because the first and essential step to replace a high fidelity model with a ROM is to construct a reliable full LTI model. The full LTI model should be sufficiently accurate when compared with building energy simulation software. The following section describes a formula to build such a LTI model from building parameters.

3.1. *Full LTI model for Building Envelope System*

The LTI model formulation of Kim and Braun (Kim and Braun 2012, 2015) that converts a complex building thermal network (see Figure 2) to a LTI system quadruple (A, B, C, D) is adopted and is briefly summarized in this section. The methodology considers heat flows of a complex building

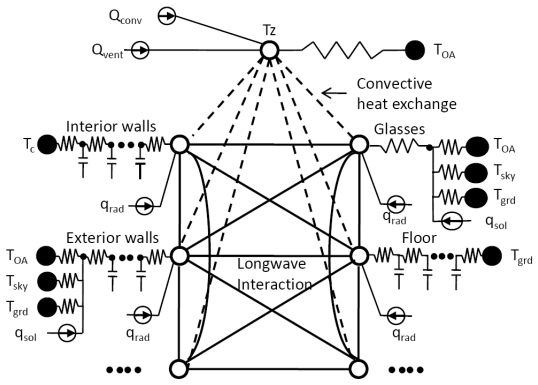

Figure 2. Thermal network unit (Kim and Braun 2015); see appendix for each nomenclature

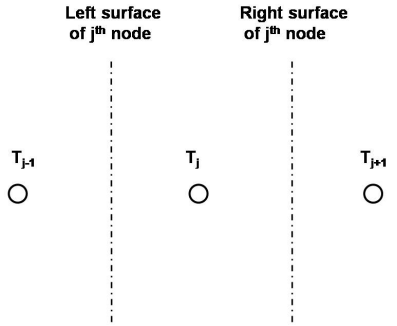

Figure 3. Notation for conduction through walls

thermal network as depicted in Figure 2. Some of the important assumptions used to construct the network unit are:

- The temperature of each surface or surface segment and of its cross section is uniform.
- A room is well-stirred.
- Each wall emits or reflects diffusely and is gray and opaque.
- Air is nonparticipating media to radiation.
- Heat transfer is one dimensional.
- Conduction between window and window frame is neglected (1-D assumption)

The main approach to develop a full LTI model is from the complex thermal network is to linearize long-wave radiation exchange and group the states (temperatures) and fundamental equations in the form of a state-space representation. For clarification, fundamental energy balance equations are shown in this paper. We refer to Kim and Braun (2015) for more detailed descriptions.

A finite volume formulation is used to describe the heat conduction through walls. Notations for the formation are shown in Figure 3. For any j^{th} node in a wall except the first and last nodes, an energy balance leads to

$$\rho_j^i C_j^i w_j^i \frac{dT_j^i}{dt} = h_{cd}^L|_j^i T_{j-1}^i - (h_{cd}^L|_j^i + h_{cd}^R|_j^i) T_j^i + h_{cd}^R|_j^i T_{j+1}^i + q_{gen,j}^i \quad (1)$$

where $h_{cd}^L|_j^i = k^L|_j^i / w^L|_j^i$ represents the heat transfer coefficient between the j^{th} and the $(j-1)^{th}$ nodes. $k^L|_j^i$ is thermal conductivity at the left surface of the j^{th} node in the i^{th} wall, $w^L|_j^i$ is distance from the $(j-1)^{th}$ node to the j^{th} node in the i^{th} wall, and $q_{gen,j}^i$ is an energy source (W/m^2) inside the j^{th} finite control volume that belongs to the i^{th} wall. ρ_j^i and C_j^i are density and

thermal capacitance at the j^{th} node in the i^{th} wall, respectively.

For any i^{th} outside wall (connected to the external ambient) belonging to an individual zone, the heat balance equation at the surface is

$$\rho_1^i C_1^i w_1^i \frac{dT_1^i}{dt} = h_{cv,ex}^i (T_a - T_1^i) + h_{cd}^R|_1^i (T_2^i - T_1^i) + \alpha_1^i q_{SW}^i + q_{LW}^i, \tag{2}$$

where T_1^i represents the wall temperature of the first node which is set to be an outside surface of the wall. q_{SW}^i and q_{LW}^i represent short wavelength solar irradiation and net long wavelength radiation exchange with the environment, respectively. $h_{cv,ex}$ is a convective heat transfer coefficient at the outside surface of a wall and T_a is outdoor air temperature, respectively. α_1^i is solar absorbance for the external surface of the i^{th} wall.

With the assumptions that the outside surface is gray and diffuse and the air is a non-participating radiation media, the net long wavelength interactions with the environment can be expressed as

$$q_{LW}^i = \sigma \epsilon_1^i F_{sky}^i (T_{sky}^4 - T_1^{i4}) + \sigma \epsilon_1^i F_{grd}^i (T_{grd}^4 - T_1^{i4}), \tag{3}$$

where σ, ϵ and F are Stefan-Boltzmann constant, emittance and view factor, respectively. Using a linear approximation of the long-wave heat exchange term gives

$$\rho_1^i C_1^i w_1^i \frac{dT_1^i}{dt} = -(h_{cv,ex}^i + h_{cd}^R|_1^i + h_{rad,ex}^i) T_1^i + h_{cv,ex}^i T_2^i + q_1^i, \tag{4}$$

where $h_{rad,ex}^i = 4\sigma\epsilon_1^i (F_{sky}^i \bar{T}_{sky}^3 + F_{grd}^i \bar{T}_{grd}^3)$, $\bar{T}_{sky} = (T_{sky} + T_1)/2$, $\bar{T}_{grd} = (T_{grd} + T_1)/2$ and $q_1^i = h_{cv,ex}^i T_a + 4\sigma\epsilon_1^i (F_{sky}^i \bar{T}_{sky}^3 T_{sky} + F_{grd}^i \bar{T}_{grd}^3 T_{grd}) + \alpha_1^i q_{SW}^i$.

The mean temperatures for long-wave exchange between the surface and sky and surface and ground are assumed to be the same for all outside surfaces.

For the I^{th} zone and i^{th} wall, the energy balance equation for the inside surface is

$$\rho_n^i C_n^i w_n^i \frac{dT_n^i}{dt} = h_{cv,in}^i (T_z - T_n^i) + h_{cd}^L|_n^i (T_{n-1}^i - T_n^i) - q_{net,rad}^i, \tag{5}$$

where $q_{net,rad}^i$ is net radiative flux out of the inside wall. The radiosity method is utilized to express the net flux assuming the walls are gray, diffuse and opaque. The same linearization method used in Eqn. 3 is employed leading to

$$\vec{q}_{net,rad} = \tilde{A}^{-1} [\tilde{B} \vec{T}_n - \vec{h}_o], \tag{6}$$

where $\tilde{A}_{ij} = \frac{\delta_{ij}}{\epsilon_j} - \frac{\rho_j}{\epsilon_j} F_{ij}$, $\tilde{B}_{ij} = 4\sigma(\delta_{ij} - F_{ij})\bar{T}^3$. F_{ij} is view factor from i to j surface, δ is the Kronecker delta, ρ is reflectance and $\vec{h}_o$ is external radiative source. A similar formulation for the treatment of long-wave interactions is shown in Modest (2003). In Eqn. 6, radiosity does not appear explicitly, which is convenient for building simulation. Since the i^{th} component of $\vec{h}_o$ represents an external radiative source acting on the i^{th} surface, the effects of internal sources and transmitted solar energy through windows are treated in a consistent manner. For any shaped room, the net radiative flux can be explicitly calculated as a function of surface temperatures if the view factors and the external radiative sources are known.

Since equations of (1), (4) and (5) for all nodes for all walls together with the zone air balance are linear, a LTI model can be developed for each zone. To treat mass-less wall layers, e.g. insulator, either an exact approach such as Ghiaus (2013) or a simpler approach which assigns arbitrary

small values to ρ_j^i or C_j^i is needed[2]. Then, a LTI model for a multi-zone building is constructed from the zonal LTI models with *connectivity* information (e.g. the I^{th} zone, the i^{th} outside wall are connected to the J^{th} zone, the j^{th} outside wall). This multi-zone LTI model includes a *doubly bordered block diagonal* matrix where the off-diagonal blocks indicate the thermal coupling between zones. For more detailed descriptions, refer to (Kim and Braun 2015).

The final LTI model for a multi-zone building has the following standard form.

$$G_o : \begin{cases} \dot{x}(t) = Ax(t) + Bu(t) \\ y(t) = Cx(t) + Du(t). \end{cases} \tag{7}$$

3.2. *Introduction of Moment Matching Problem and Krylov Subspace Method*

The Krylov subspace method is originated from the eigenvalue problem for a large system in the field of mathematics and numerical analysis, and there are a variety of different algorithms (for more descriptions of algorithms for the eigenvalue problem, see (Sorensen 1997; Dahlquist and Björck 1974)). Therefore, full understanding of the method and algorithms would require an intensive mathematical background and significant time. In this paper, the focus is on describing the key concepts to provide a key concept, overall issues of the moment matching problem, and an overall work flow of the Krylov subspace method showing how this method solves the moment matching problem. We refer to the textbook of Antoulas (2005) for rigorous descriptions of various MOR algorithms, and Gugercin (2003); Salimbahrami and Lohmann (2002) for the moment matching problem and Krylov subspace method. It is assumed that the system quadruple of an LTI dynamic system, (A, B, C, D), is available.

The problem definition of MOR for a LTI system is to construct lower order matrices for Eqn. 9, from the original system of Eqn. 8.

$$G_o : \begin{cases} \dot{x}(t) = Ax(t) + Bu(t) \\ y(t) = Cx(t) + Du(t) \end{cases} \tag{8}$$

$$G_r : \begin{cases} \dot{x_r}(t) = A_r x_r(t) + B_r u(t) \\ y_r(t) = C_r x_r(t) + D_r u(t) \end{cases} \tag{9}$$

where the state $x(t) \in \mathrm{R}^n$, $x_r(t) \in \mathrm{R}^r$ and $r \ll n$. In other words, we want to reduce the state dimension from n to r while maintaining the original input-output relation as much as possible.

To explain the moment matching (MM) problem, consider *the Laurent series expansion* of a transfer function $G(s) = C(sI - A)^{-1}B + D$ in the neighborhood of s_0 in a complex plane.

$$G(s) = \eta_0(s_0) + \eta_1(s_0)(s - s_0) + \cdots + \eta_k(s_0)(s - s_0)^k + \cdots \tag{10}$$

where η_j is called the j^{th} moment of G at s_0. It is assumed that there are no poles within a neighborhood of s_0.

The MM problem is to construct (A_r, B_r, C_r, D_r) such that the first k moments of G_r, denoted as $\eta_{r,0}(s_0), \eta_{r,1}(s_0), \cdots, \eta_{r,k-1}(s_0)$, exactly match those of G_o, i.e. $\eta_{o,0}(s_0), \eta_{o,1}(s_0), \cdots, \eta_{o,k-1}(s_0)$. A conceptual figure of the MM problem is shown in Figure 4. Compared with the balance truncation method, the moment matching problem at a single point is essentially a local approximation problem of a function.

[2]The latter approach is adopted in this paper for the simplicity

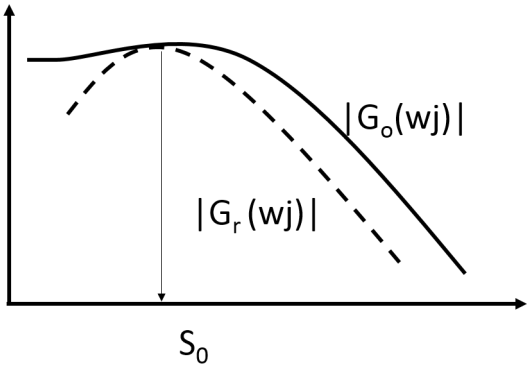

Figure 4. Conceptual diagram of the Moment Matching Problem

Since the moments have different expressions of the system quadruple (A, B, C, D) at different center points, i.e.

$$\eta_0(s_0) = D, \quad \eta_j(s_0) = CA^{(j-1)}B\,, \qquad if \quad s_0 = 0 \tag{11}$$

$$\eta_0(s_0) = -D, \quad \eta_j(s_0) = -CA^{-j}B, \qquad if \quad s_0 = \infty \tag{12}$$

$$\eta_0(s_0) = -D, \quad \eta_j(s_0) = -C(A - s_0 I)^{-j}B \qquad if \quad s_0 \notin \{0, \infty, \Lambda(A)\} \tag{13}$$

where $\Lambda(A)$ is the spectrum of A, the MM problem becomes one of finding (A_r, B_r, C_r, D_r) such that

$$C_r {A_r}^{(j-1)} B_r = CA^{(j-1)}B \;\; , (\forall j \in \{1, 2, \cdots, k\}), \qquad if s_0 = 0 \tag{14}$$

$$C_r {A_r}^{-j} B_r = CA^{-j}B \;\; (\forall j \in \{1, 2, \cdots, k\}), \qquad if s_0 = \infty \tag{15}$$

$$C_r (A_r - s_0 I)^{-j} B_r \;\; = C(A - s_0 I)^{-j}B \;\; (\forall j \in \{1, 2, \cdots, k\}), \; if s_0 \notin \{0, \infty, \Lambda(A)\} \tag{16}$$

The MM problems at $s_0 = 0, s_0 = \infty$ and $s_0 \notin 0, \infty, \Lambda(A)$ are known as *Padé approximation*, *partial realization* and *rational interpolation problems*, respectively.

The Krylov subspace method is one of the most numerically efficient and stable algorithms for the MM problem. It seeks a lower dimensional subspace namely the Krylov subspace where 1) original dynamics are projected onto and 2) partial moments of the projected dynamic system equate to those of the original dynamic system.

In order to show how the Krylov subspace method works, consider a simple case, the partial realization problem ($s_0 = \infty$) for a single input system that is $B \in \mathrm{R}^{n \times 1}$. Solution steps of the Krylov subspace method may be described in the following three steps.

Step 1 : **Define Krylov subspace(s)**
Given the system (A, B, C), define a (input) Krylov subspace as follows.

$$\mathcal{K} := span\, col\, [B, AB, \cdots, A^{-k}B] \tag{17}$$

where span col represents the column span, i.e. $\mathcal{K}$ is the space spanned by column vectors of the matrix $[B, AB, \cdots, A^{-k}B]$.

Step 2 : **Define basis of a Krylov subspace**
Define $V \in \mathrm{R}^{n \times k}$ as a basis of $\mathcal{K}$ (in the form of a matrix) and choose any $W^T \in \mathrm{R}^{k \times n}$ as a left inverse of V, i.e. $W^T V = I$.

Step 3 : **Project original dynamics on the subspace**
Construct the reduced order system matrices (A_r, B_r, C_r, D_r) by *the Petrov-Galerkin projection* with V and W. That is,

$$A_r = W^T AV, B_r = W^T B, C_r = CV, D_r = D. \tag{18}$$

The key point is that the resulting (A_r, B_r, C_r, D_r) is able to match up to the k^{th} moment. To see this, consider the first moment of G_r at $s_0 = \infty$. It is $\eta_{r,1}(\infty) = C_r B_r = (CV)(W^T B)$. From the definition of the Krylov subspace (see the 1^{st} step, Eqn. (17)), B can be expressed as $B = V\zeta$ for some $\zeta \in \mathrm{R}^r$. Therefore, $C_r B_r = (CV)(W^T B) = (CV)(W^T V\zeta) = CV\zeta = CB$. The biorthorgonal condition of $W^T V = I$ is used in the derivation. This shows the first moments of G_r and G_o are equal. Now consider $\eta_{r,2}(\infty) = C_r A_r B_r$. Using Eqn. (18), $\eta_{r,2}(\infty) = CV \cdot W^T AV \cdot W^T B$. Again there exists $\zeta(\in R^r)$ s.t. $B = V\zeta$. Therefore $\eta_{r,2}(\infty) = CV \cdot W^T AB$. Since $AB \in \mathcal{K}$ from the definition of the Krylov subspace, it can be also expressed as $AB = V\zeta'$ for some $\zeta'(\in \mathrm{R}^r)$. This leads to $\eta_{r,2}(\infty) = CV\zeta' = CAB = \eta_{o,2}(\infty)$. By applying the same process, it can be shown that the Krylov subspace method is able to match up to the k^{th} moment.

Although the partial realization problem for a single input system is used for simplicity, the procedure solves more complex moment matching problems with different choices of a Krylov subspace in the 1^{st} step. For example, for the rational interpolation problem, we define a Krylov subspace as follows.

$$\mathcal{K} := span\ col\,[(s_0 I - A)^{-1} B, (s_0 I - A)^{-2} B, \cdots, (s_0 I - A)^{-k} B]. \tag{19}$$

The different choice is from the fact that moments are expressed differently as shown in Eqn. (11). It can be proven that the steps of the Krylov subspace of Eqn. (19) solve a rational interpolation problem.

The remaining problem for the Krylov subspace method is how to construct V and W in a numerically efficient manner in the 2^{nd} step. Ideally, the *Gram-Schmidt process* (or QR factorization) can be applied to form a basis of the Krylov subspace, but it is not numerically reliable since $(s_0 I - A)^{-j} B$, for the rational interpolation problem as an example, converges very quickly to the largest eigenvector as the exponent j increases, resulting in a badly conditioned matrix. To understand this numerical issue, it is helpful to recall that *the Power method* approximates the largest eigenvalue and eigenvector of a matrix. Therefore, for generating a numerically reliable basis V of a Krylov subspace, the *Arnoldi or Lanczos algorithms* are typically used rather than the Gram-Schmidt process (Householder 2006). Like the QR factorization, the Arnoldi method sequentially generates an orthonormal basis for an updated column vector (for single input systems) by perpetually projecting it onto the subspace spanned by the previous orthonormal basis. However, for the method, the updated vector is not the multiplication of the matrix power of $(s_0 I - A)^{-j}$ with B, but is the multiplication of $(s_0 I - A)^{-1}$ with the latest orthogonal basis which allows avoiding the numerical issue of the Gram-Schmidt process.

The Arnoldi algorithm for the rational interpolation problem for a single input system can be expressed as follows (Antoulas 2005). v_j represents the j^{th} orthonormal basis with respect to a previous orthonormal basis set contained in the j^{th} Krylov sequence, i.e. $(A - s_0 I)^{-j} B$. For the Arnoldi algorithm, W is equal to V. Since V as a result of the Arnoldi algorithm is an orthonormal basis for a Krylov subspace, the biorthonormality condition of $W^T V = I$ in the 2^{nd} step is automatically satisfied.

3.3. *Solution of applying the Krylov Subspace Method for Building Applications*

It is important to mention that there are a variety of different choices for the 1^{st} and 2^{nd} steps to solve a MM problem resulting in a large number of approaches In addition, there are several technical issues in applying the Krylov method for multi-zone buildings applications. That is, not

Algorithm Arnodi algorithm for a rational interpolation problem (single input system)

inputs: $(A, B), s_0, k$
outputs: V, W^T

Solve $(A - s_0 I)v_1 = B$.
$v_1 \leftarrow v_1/||v_1||$.
$V \leftarrow v_1$.
Solve $(A - s_0 I)w = v_1$.
$p_1 = (I - VV^T)w$.
  for $1 \leq j \leq k - 1$ **do**
    $v_{j+1} = p_j/||p_j||$
    $V \leftarrow [V, v_{j+1}]$
    Solve $(A - s_0 I)w = v_{j+1}$
    $p_{j+1} = (I - VV^T)w$
  end for
$W^T = V^T$

all MM approaches in the MOR literature are suitable for handling large-scale buildings and one has to be carefully selected.. In this section, we present a complete solution , i.e. a choice of algorithms, to handle those issues for generating a ROM for large scale buildings, which is one of the main contribution of this paper.

3.3.1. Algorithm to handle general a MIMO structure

For building applications, the Krylov subspace method should handle general multi-input multi-output (MIMO) systems because building dynamics are driven by various indoor and outdoor heat sources and have a number of outputs which could be zone air temperatures or heating/cooling loads depending on an application.

The Arnoldi algorithm is preferable for building applications compared with the Lanczos algorithm because of the difficulty and complexity of the Lanczos procedure for general MIMO systems that are non-symmetric and have different numbers of inputs and outputs, i.e. $m \neq p$, (Gugercin 2003).

For the MIMO case, one may attempt to extend the Anordi algorithm for SISO systems shown in the previous section by simply treating the matrix B as a block of vectors. In this case, the updated coordinate, v_j, will be a matrix rather than a vector. However, this approach could fail because it may yield rank deficiency and redundancy in the projection matrices (Gugercin 2003). More precisely, the resulting V may be not a full rank such that $V^T V \neq I$. Therefore, modification(s) of the Arnordi algorithm must be made for an appropriate deflation of V for MIMO systems. We adopt the method proposed by Boley (1994) to overcome this challenge. In this method, block vectors are updated without considering rank deficiency and the deflation is made by using the Gram-Schmit process and a rank revealing process at each iteration of the Arnodli procedure. We present the following algorithm which is a modified version of Boley's algorithm.

The operator qr acts on a matrix and extracts only linearly independent column vectors after the QR factorization using the Gram-Schmit process of the matrix. The presented algorithm is mathematically the same as the Boley's method but numerically more efficient because it avoids an internal iteration which requires a number of matrix multiplications. The modification is helpful to further reduce the computation time for obtaining V.

3.3.2. Selection of a Krylov subspace

As mentioned, there are different Krylov spaces to the input Krylov subspace, i.e. Eqn. (17) for the partial realization problem and Eqn. (19) for the rational interpolation problem, that can also

Algorithm MIMO Arnodi algorithm for a rational interpolation problem

inputs: $(A, B), s_0, k$
outputs: V, W^T

Solve $(A - s_0 I)v_1 = B$.
$v_1 \leftarrow qr(v_1)$. # rank deflation and scale
$V \leftarrow v_1$.
Solve $(A - s_0 I)w = v_1$. $p_1 = (I - VV^T)w$.
  for $1 \leq j \leq k-1$ **do**
    $v_{j+1} = qr(p_j)$ # rank deflation and scale
    $V \leftarrow [V, v_{j+1}]$
    Solve $(A - s_0 I)w = v_{j+1}$
    $p_{j+1} = (I - VV^T)w$
  end for
$W^T = V^T$

solve the same MM problem. A different choice would result in different numerical computation and performance. Therefore, in order to apply the Krylov method to buildings, an appropriate Krylov subspace should be defined. It turns out the choice of the input Krylov subspace could lead to poor performance for large size buildings. This is because there are many inputs for a building envelope system that include internal heat gain for each zone, solar irradiation for each orientation of an external wall, direct and diffuse parts of transmitted solar radiations for each type and orientation of a window. Since, in order to match the first k^{th} moments, the state dimension r of a reduced system is required to be around $k \times m$, the resulting ROM projected onto the input Krylov subspace still has a high dimension for a given k. On the other hand, if we enforce r to be small, the condition of $r \approx k \times m$ implies that k needs to be small resulting in a poor accuracy of the ROM. This problem can be overcome simply but effectively by using the output Krylov subspace (or extended observability matrix) which is defined for a rational interpolation problem by

$$\mathcal{K} = span\ col\,[(s_0 I - A^T)^{-1}C^T, (s_0 I - A^T)^{-2}C^T, \cdots, (s_0 I - A^T)^{-k}C^T]. \tag{20}$$

To construct an orthonormal basis for the output Krylov subspace, the presented MIMO Arnoldi algorithm can be used with inputs of (A^T, C^T).

3.3.3. Handling multiple interpolation points

For many situations, dynamics of building envelope system in both low and high frequency ranges are of interest: Matching in a low frequency range is important for building load calculation under a fixed setpoint and matching in a high frequency range associated with zone air dynamics is important for control applications. Therefore, it is of interest to match moments at multiple frequency points to have increased reliability as depicted in Figure 5. In the framework of the MM problem, it is equivalent to obtain G_r of which

$$\begin{aligned} \eta_{r,i}(s_0) &= \eta_{o,i}(s_0) \quad \forall i \in \{0, 1, \cdots, k_0\}, \\ \eta_{r,j}(s_1) &= \eta_{o,j}(s_1) \quad \forall j \in \{0, 1, \cdots, k_1\}, \\ &\cdots \end{aligned} \tag{21}$$

for some $k_0, k_1, \cdots$.

Fortunately, the Krylov subspace method can easily handle this MM problem. It is well known that a dynamic model projected onto the unions of all Krylov subspaces associated with $s_0, s_1, \cdots,$

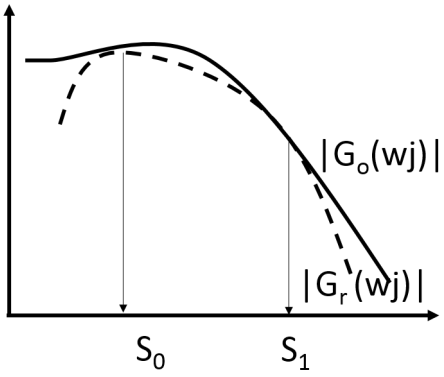

Figure 5. Conceptual diagram of the Moment Matching Problem at multiple points

can meet the goal of matching moments at multiple points. More precisely, the rational interpolation problem at multiple points can be solved by finding a set of basis of the Krylov subspace defined at each point.

3.3.4. Final algorithm

The final algorithm that we propose combines the algorithms above from Section 3.3.1 to 3.3.3, and is compactly presented below.

Algorithm Final algorithm

inputs: $A, C, s_0, s_1, \cdots, s_n, k_0, \cdots, k_n$
outputs: V, W^T

V = empty matrix # initialization
  for $1 \leq i \leq n$ **do**
    $V_i = MIMOArnoldi(A^T, C^T, s_i, k_i)$
    $V \leftarrow [V, V_i]$
  end for
$V \leftarrow qr(V)$

"MIMOArnoldi" is the block Arnoldi algorithm presented in Section 3.3.1. Once V, W^T is defined after the final algorithm, the ROM can be obtained by performing the Petrov-Galerkin projection, i.e. Eqn. (18).

4. Case Study

4.1. *Comparison between Balanced Truncation Method and Krylov Subspace Method*

Although characteristics of the balanced truncation method and Krylov subspace method have been studied in the literature, we present a simple numerical experiment result to illustrate numerical behaviors of the methods for the readers who are not familiar with MOR. An arbitrary stable SISO LTI model, denoted as $G_o := (A, B, C, D)$, was generated by a random continuous test model generator, rss, in MATLAB. A is a $n \times n$ matrix. To ensure all poles are located on the left half plane, the *Gershgorin circle theorem* (Meyer 2000) was used to adjust diagonal entities of the A matrix. ROMs were generated from the balanced truncation method and the Krylov subspace method.

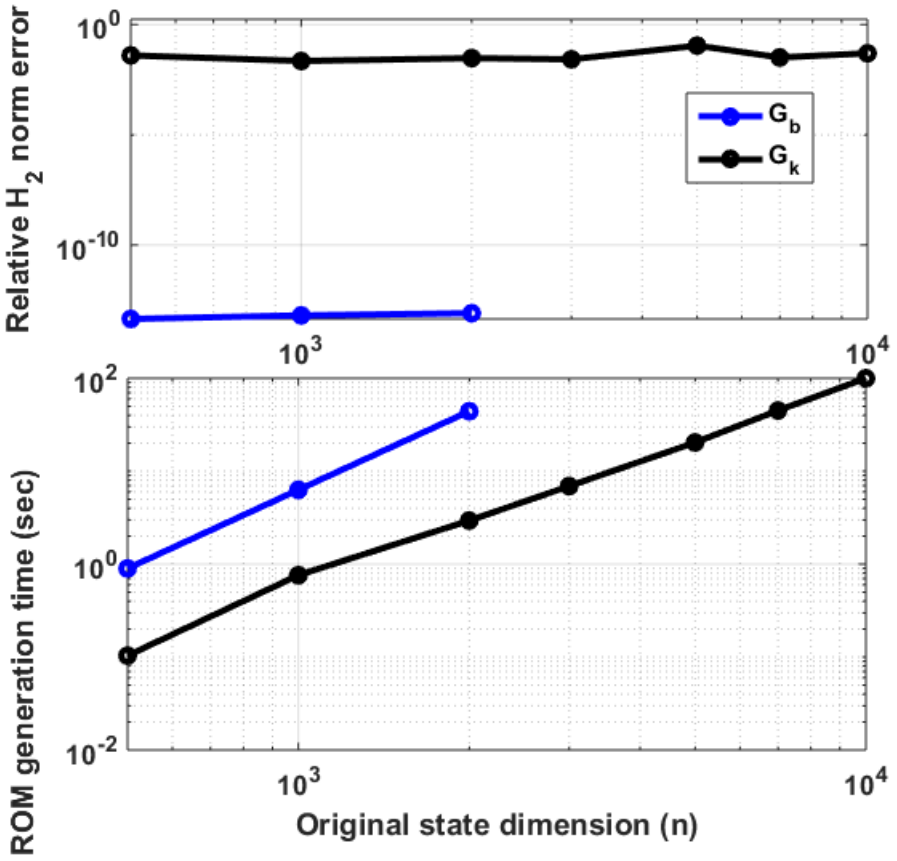

Figure 6. Numerical test comparisons between the balanced truncation method and Krylov subspace method for arbitrary stable systems

Reduced-order dimensions r were set to 100 for both approaches, and s_0 was set to 10^{-2} for the Krylov subspace method. As an accuracy measure, a relative H_2 norm error, defined below, was used to measure the truncation error.

$$Relative H_2 \ norm \ error := \frac{||G_o - G_r||_2}{||G_o||_2} \tag{22}$$

where $||G||_2 := \sqrt{1/2\pi \int_{-\infty}^{\infty} Trace(G(jw)^* G(jw))dw}$ for all stable transfer functions, G. The subscripts, o and r, represent the original and the reduced system, respectively.

All numerical experiments were run with MATLAB version R2010a on a desktop computer with a quad core 3.10 GHz CPU, 3.16 GB RAM and Windows 32- bit systems. The memory available for MATLAB was 791 MB.

Figure 6 shows comparisons of the relative norm errors and ROM generation times for various n. (G_b, G_k) represent ROMs for the balanced truncation and Krylov methods, respectively. In the first subfigure, the H_2 norm errors of G_b are very small ($< 10^{-10}$). This is because the Hankel singular values for many systems decay extremely rapidly and the specified r ($= 100$) is sufficiently high enough. On the other hand, the H_2 norm errors of G_k are much higher within $[0.026, 0.110]$ even with the same r. This confirms that the balanced truncation method is superior to the Krylov method in terms of global accuracy. However, the computing times to generate ROMs for the balanced truncation method are much higher than those of the Krylov method as shown in the

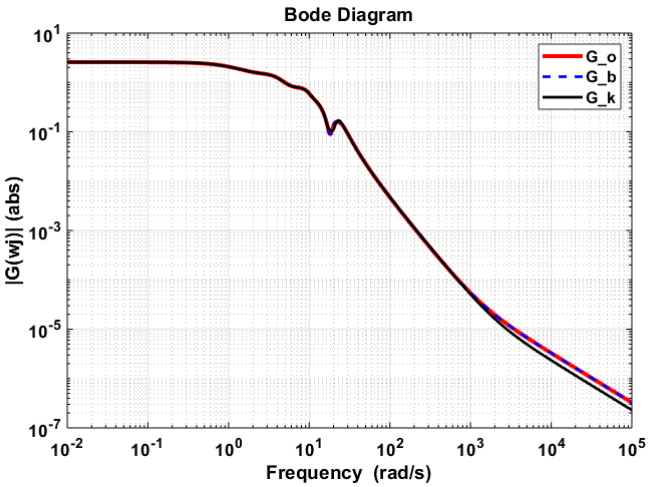

Figure 7. Bode magnitude plot comparisons between true and reduced-order models

Table 1. Comparisons between two MOR methods

	Balanced	Krylov
Numerical cost (flops)	$O(n^3)$	$O(r^2n)$
Range of applicability	up to order few thousand	up to several ten/hundred thousands
Iterative method	No	Yes
Numerical reliability for large n	No	Yes
Accuracy of the reduced system	More	Less
Preserving stability	Yes	No
Reliable stopping criterion	Yes	No

second subfigure. More importantly the balanced truncation method could not be applied when n was over about two thousand due to excessive memory requirements. However, the Krylov method was applicable for a ten thousand state without causing any issues with reasonable computing times as shown in the figure. This is because the balanced truncation method computes exact solutions of the two Lyapunov equations, i.e. reachability and observability grammians, requiring dense computations, and therefore can be carried out for systems of a modest dimension. On the other hand, the Krylov subspace method is iterative in nature and hence can be applied to very high order systems.

The poorer accuracy of G_k compared with G_b should not be exaggerated. Figure 7 shows comparisons of the Bode magnitude plots for $n = 500$. As indicated by the H_2 norm error, G_b is very close to G_o with negligible errors over all frequency range. On the other hand, G_k perfectly match to G_o nearby the specified local frequency point $s_0 = 10^{-2}(rad/s)$ but has some errors for a higher frequency region. The errors do not look significant in the bode plot and G_k should be sufficiently accurate for many situations.

Table 1 from Salimbahrami (2005) summarizes general comparisons between the two MOR approaches. Except for reduced computational loads, there are no advantages of the Krylov subspace method regarding the quality of a reduced-order model. Therefore, the balanced truncation method should be considered first for model-order reduction. However, when a system of interest is very large such that the balanced truncation method is *impossible* to apply due to a limited source of computing power (see the case study below), the Krylov subspace method should be utilized.

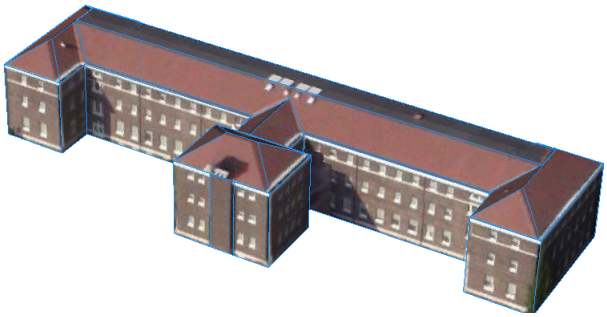

Figure 8. External view of Building 101 (3D Google Map)

4.2. *Case Study Results and Discussion*

4.2.1. Case study building description

For testing the validity of the process from the TRNSYS input file interface to the reduced-order LTI model generator, dynamic responses of a ROM and TRNSYS model for a multi zone building were compared. A multi-zone (59-zone) commercial building located at the Philadelphia Navy Yard was used to test feasibility and performance with respect to the accuracy and computational requirements. Figure 8 shows an external view of the building. Some characteristics used in the modeling include:

- 55,000 square feet of total floor area
- 3 occupied floors with a basement and attic spaces and a total of 59 zones
- 18 different types of layers used for wall construction that primarily consist of concrete, insulation board, plaster board, and brick
- window-area ratio: about 20%
- 6 different types of walls having various combinations of the layer types
- TMY2 weather data for Philadelphia
- Values of 17.77 [W/m2-K] and 3.05 [W/m2-K] were used for convective heat transfer coefficients at the outside and inside surfaces, respectively

The original LTI model (G_o) which predicts building heating/cooling load profiles of individual zones under responses of indoor and outdoor conditions was developed through a TRNSYS interface and LTI model generator shown in Figure 1. The TRNSYS interface is to extract necessary building parameters from a TRNSYS model input file, *.bui, to automatically construct a full LTI model described in Section 3.1. This tool allows handling general building models which consist of thousands of parameters. For more information about the tool, refer to Kim et al. (2018).

The 59-zone model has 59 outputs (p) for zonal building loads, and 151 inputs (m) including internal gain for each zone, outdoor air temperature, sky temperature, ground temperature, solar irradiation depending on building surface orientations, and transmitted direct and diffuse solar irradiation depending on window orientations and types. The state dimension (n) is over 4000.

The final algorithm presented in Section 3.3.4 was applied to G_o with two frequency points $s_0 \approx 0$ and $s_1 = 1/(60 \times 10)$ and k=3. A resulting ROM (G_r) had the state dimension of $r = 354$. The point $s_0(\approx 0)$ captures DC-gains of G_o which are critical for building load calculations under a fixed temperature setpoint. On the other hand, s_1 is to capture faster dynamic responses , e.g. weather or internal gain profiles.

The computing times for each step of the process are shown in Table 2. All computation times are based on a quarter-core 3.10 GHz with 3.16 GB memory desktop computer. The time required to extract parameters from a BES input file and to form the full LTI model is negligible: It took only one sec to build the entire system matrices. The ROM generation took the majority of the processing time. However, it should be noticed that it is not feasible to apply the balanced

Table 2. Computation times for interface, and full and reduced order LTI model generators for a 60-zone building

	Interface	LTI generator	ROM generation
Computation time (sec)	0.70	0.35	58.52

Table 3. A one-year simulation time comparisons for a 59-zone building

	TRNSYS	ROM	Computation time savings
computation time (sec)	241.39	1.06	99.56 (%)

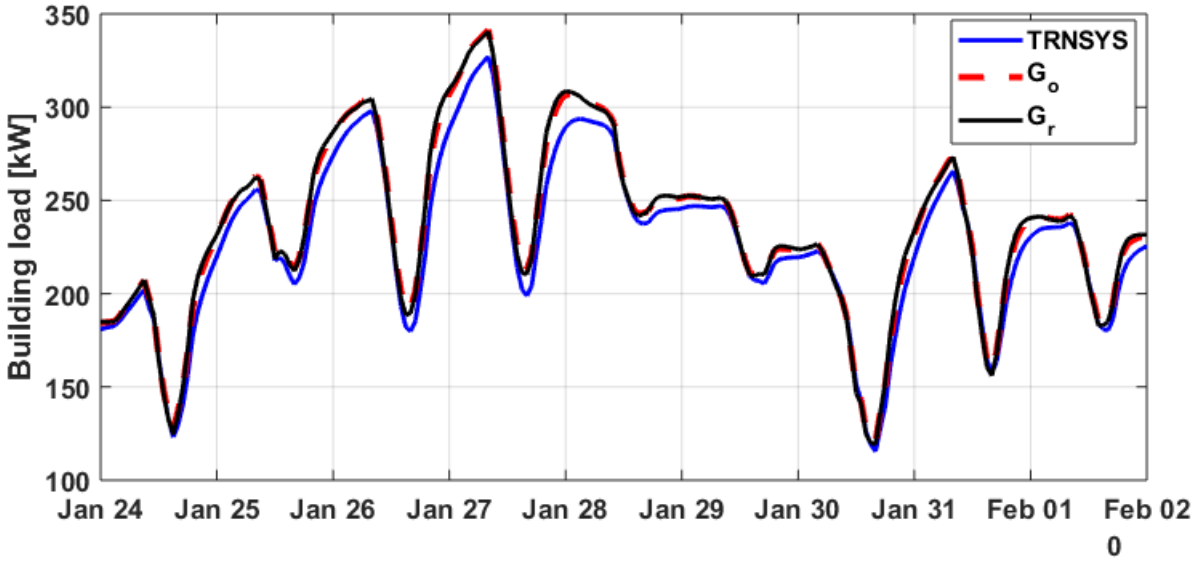

Figure 9. Load comparisons between TRNSYS and full-order models for a heating period (heating (+), cooling (-))

truncation method for this application due to the high dimensionality.

A one-year simulation time comparison between TRNSYS and the ROM is provided in Table 3. They are 241.38 sec for TRNSYS and 1.06 sec for the ROM. Note that computational time for solution of differential equations is highly dependent on the differential or difference equation solver algorithm. The computational times are based on an ODE (ordinary differential equation) solver of MATLAB. Performance judgment with respect to simulation time relative to TRNSYS is difficult. Furthermore, one of the most important differences between the state-space representation and TRNSYS is that the former is continuous, but the latter is represented using discrete equations. Therefore, the time comparisons could vary depending on solver algorithms, but the ROM provides a factor of 100 faster computation for various ode solvers.

The total computation time that includes everything associated with the ROM generation and simulation is interesting especially for a parametric study, e.g. retrofit analysis, and building design optimization. The approach still gives significant time savings of 75.32 % and is around 4 times faster. This is because the reduction in computation time for annual simulation is much greater although the ROM generation time seems to be significant. The results indicate that there are significant computation time savings potential utilizing the Krylov subspace method for building simulations of large-scale buildings, if G_r is accurate enough.

Sample model output comparisons between TRNSYS, G_o and G_r are shown in Figure 9 to 11 which show example comparisons of total building load profiles for peak heating days, mild days, and peak cooling days, respectively. The setpoints for all zones were set to 23 ^oC in calculating

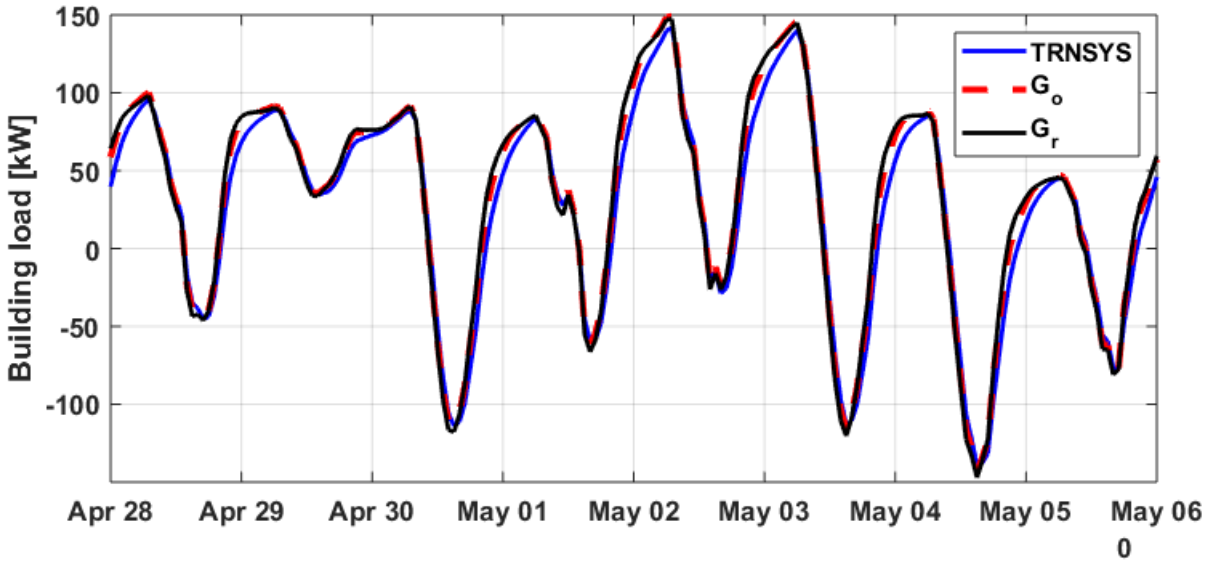

Figure 10. Load comparisons between TRNSYS and full-order models for a mild period (heating (+), cooling (-))

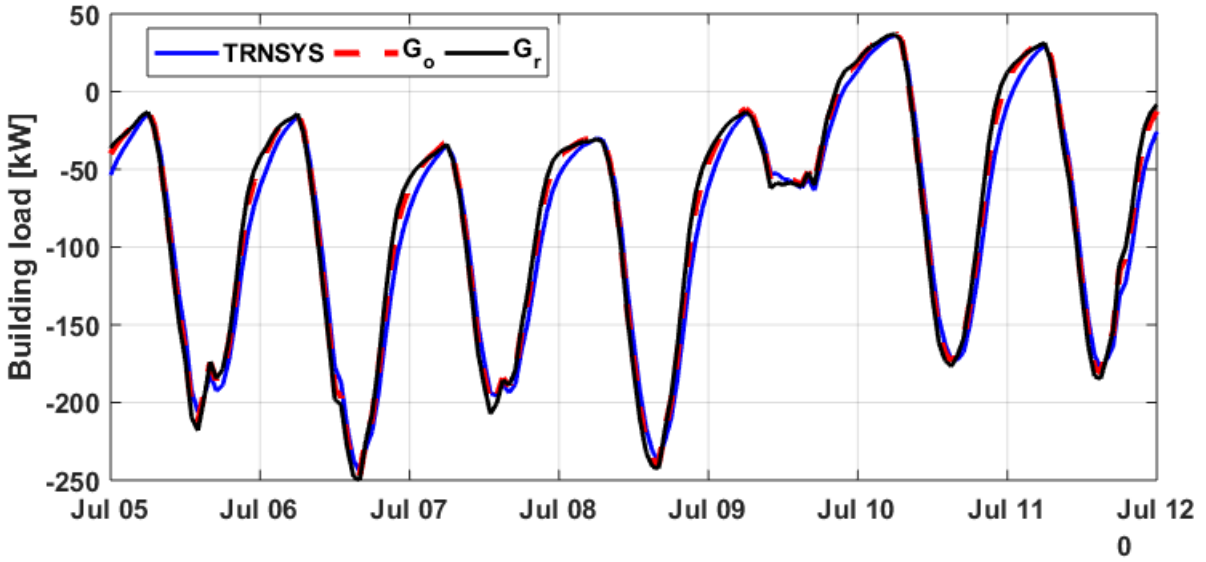

Figure 11. Load comparisons between TRNSYS and full-order models for a cooling period (heating (+), cooling (-))

buildings loads. It can be confirmed that G_o and G_r are almost identical. There are differences between G_r and TRNSYS results, especially for the heating season. Through parametric study, the differences were found to be associated with the treatment of windows in the full LTI model. It is expected that these differences could be mostly eliminated by using a consistent approach for the windows. Nonetheless, the fulll LTI model and ROM clearly capture major dynamics of the baseline building load.

Overall performance comparisons are summarized in Table 4. Together with Table 2 and 3, the case study results demonstrate that the proposed Krylov subspace algorithm together with the overall work flow works efficiently and accurately with differences of less than 5% compared to TRNSYS.

Table 4. Comparisons of predicted building load for one-year simulation

	TRNSYS	G_o	G_r	Relative ERR of G_r w.r.t. TRNSYS [%]
Peak heating load [kW]	327.20	341.56	340.65	4.11
Peak cooling load [kW]	244.72	247.18	249.99	2.15
Annual heating load [MWh]	771.69	808.78	810.00	4.96
Annual cooling load [MWh]	183.76	175.02	176.22	4.09

5. Conclusions

The balanced truncation method which is one of the most popular and reliable model order reduction methods in the literature is computationally very demanding or not feasible for application to large-scale buildings. This paper introduced an alternative method, the Krylov subspace method, to the building energy simulation field that can effectively and reliably reduce high dimensional building dynamics. A complete algorithm from the literature of control and numerical analysis was identified, modified and presented for building applications. A case study for a 60-zone building was carried out. In this study, the lower order model gave results that were about a factor of 100 reduction in computational time compared to a conventional building energy simulation software but with differences less than 5%. The differences were primarily due to differences in the way windows were treated and not due to the reduced-order modeling approach. The computational requirements for generating the ROM are small enough such that this approach would be useful for general building simulations, particularly when considering parametric studies, optimization for design and control assessment where a number of iterations for a long term energy simulation is required.

Nomenclature

LTI linear time invariant system
MOR model order reduction
ROM reduced order model
SISO single input single output LTI system
MIMO multi input multi output LTI system
n state dimension of an original LTI system
r state dimension of a reduced original LTI system
m the number of inputs for a LTI system
p the number of outputs for a LTI system
G_o transfer function for an original LTI system
G_r transfer function after a model order reduction
η_o coefficients of the Laurent series expansion of G_o
η_r coefficients of the Laurent series expansion of G_r
$\mathcal{K}$ a Krylov subspace
V a basis of a Krylov subspace
W a left inverse of V
s_j a complex number
k a desired number of moments to be matched
v_j a coordinate of a basis
H_2 Hardy two norm

References

Antoulas, A., 2005. Approximation of large-scale dynamical systems. volume 6. Society for Industrial Mathematics.

Antoulas, A., Sorensen, D., Gugercin, S., 2001. A survey of model reduction methods for large-scale systems. Contemporary mathematics 280, 193–220.

Boley, D.L., 1994. Krylov space methods on state-space control models. Circuits, Systems and Signal Processing 13, 733–758.

Crawley, D., Lawrie, L., Pedersen, C., Winkelmann, F., 2000. Energy plus: energy simulation program. ASHRAE journal 42, 49–56. URL: http://apps1.eere.energy.gov/buildings/energyplus/.

Dahlquist, G., Björck, Å., 1974. Numerical Methods. Prentice-Hall, Inc.

Del Barrio, E.P., Lefebvre, G., Behar, P., Bailly, N., 2000. Using model size reduction techniques for thermal control applications in buildings. Energy and Buildings 33, 1–14.

Deng, K., Barooah, P., Mehta, P.G., Meyn, S.P., 2010. Building thermal model reduction via aggregation of states, in: American Control Conference (ACC), 2010, IEEE. pp. 5118–5123. URL: http://ieeexplore.ieee.org/xpls/abs_all.jsp?arnumber=5530470.

Deng, K., Goyal, S., Barooah, P., Mehta, P.G., 2014. Structure-preserving model reduction of nonlinear building thermal models. Automatica 50, 1188–1195.

Foucquier, A., Robert, S., Suard, F., Stéphan, L., Jay, A., 2013. State of the art in building modelling and energy performances prediction: A review. Renewable and Sustainable Energy Reviews 23, 272–288.

Gao, Y., Roux, J., Zhao, L., Jiang, Y., 2008. Dynamical building simulation: A low order model for thermal bridges losses. Energy and Buildings 40, 2236–2243.

Ghiaus, C., 2013. Causality issue in the heat balance method for calculating the design heating and cooling load. Energy 50, 292–301.

Goyal, S., Barooah, P., 2012. A method for model-reduction of non-linear thermal dynamics of multi-zone buildings. Energy and Buildings 47, 332–340. URL: http://www.sciencedirect.com/science/article/pii/S0378778811006001.

Gugercin, S., 2003. Projection methods for model reduction of large-scale dynamical systems. Ph.D. thesis. Rice University.

Householder, A.S., 2006. Principles of numerical analysis. Courier Corporation.

Ioli, D., Falsone, A., Papadopoulos, A.V., Prandini, M., 2017. A compositional modeling framework for the optimal energy management of a district network. Journal of Process Control .

Kim, D., Bae, Y., Braun, J.E., Horton, W.T., 2018. A tool for generating reduced-order models from building energy simulation input files to enable optimal design and control analysis .

Kim, D., Braun, J.E., 2012. Reduced-order building modeling for application to model-based predictive control. Simuild 2012, Fifth National Conference of IBPSA-USA, Madison, Wisconsin .

Kim, D., Braun, J.E., 2015. A general approach for generating reduced-order models for large multi-zone buildings. Journal of Building Performance Simulation 8, 435–448.

Kim, D., Zuo, W., Braun, J.E., Wetter, M., 2013. Comparisons of building system modeling approaches for control system design. 13th Conference of International Building Performance Simulation Association, Chambery, France , pp. 3267–3274.

Klein, S., Beckman, W., Mitchell, J., Duffie, J., Duffie, N., Freeman, T., Mitchell, J., Braun, J., Evans, B., Kummer, J., et al., 2004. Trnsys 16–a transient system simulation program, user manual. Solar Energy Laboratory. Madison: University of Wisconsin-Madison .

Laub, A.J., 2005. Matrix analysis for scientists and engineers. volume 91. Siam.

Li, X., Wen, J., 2014. Review of building energy modeling for control and operation. Renewable and Sustainable Energy Reviews 37, 517–537.

Ménézo, C., Roux, J., Virgone, J., 2002. Modelling heat transfers in building by coupling reduced-order models. Building and environment 37, 133–144. URL: http://www.sciencedirect.com/science/article/pii/S0360132301000233.

Meyer, C.D., 2000. Matrix analysis and applied linear algebra. volume 71. Siam.

Modest, M.F., 2003. Radiative heat transfer. Academic press.

Moore, B., 1981. Principal component analysis in linear systems: Controllability, observability, and model reduction. Automatic Control, IEEE Transactions on 26, 17–32. URL: http://ieeexplore.ieee.org/xpls/abs_all.jsp?arnumber=1102568.

Palomo, E., Bonnefous, Y., Déqué, F., 1997. Guidance for the selection of a reduction technique for thermal

models, in: Proceedings of Building Simulation 97 Conference, Prague, Czech Republic.

Palomo Del Barrio, E., Lefebvre, G., Behar, P., Bailly, N., 2000. Using model size reduction techniques for thermal control applications in buildings. Energy and Buildings 33, 1–14. URL: http://www.sciencedirect.com/science/article/pii/S0378778800000608.

Picard, D., Drgoňa, J., Kvasnica, M., Helsen, L., 2017. Impact of the controller model complexity on model predictive control performance for buildings. Energy and Buildings 152, 739–751.

Plessis, G., Filfli, S., Muresan, C., Bouia, H., EnerBat, E., Moret, F., 2011. Using design of experiments methods to develop low energy building model under modelica, in: Proceedings of Building Simulation, pp. 988–995.

Salimbahrami, B., Lohmann, B., 2002. Krylov subspace methods in linear model order reduction: Introduction and invariance properties, in: Sci. Rep.. Inst. of Automation, Citeseer.

Salimbahrami, S.B., 2005. Structure preserving order reduction of large scale second order models. Ph.D. thesis. Technische Universität München.

Sorensen, D.C., 1997. Implicitly restarted arnoldi/lanczos methods for large scale eigenvalue calculations, in: Parallel Numerical Algorithms. Springer, pp. 119–165.